The Journal of Experimental Biology 214, 1836-1844

doi:10.1242/jeb.055475

RESEARCH ARTICLE

Proteomic response to elevated P_{CO_2} level in eastern oysters, *Crassostrea virginica*: evidence for oxidative stress

Lars Tomanek[1,*], Marcus J. Zuzow[1], Anna V. Ivanina[2], Elia Beniash[3] and Inna M. Sokolova[2]

[1]Department of Biological Sciences, Center for Coastal Marine Sciences and Environmental Proteomics Laboratory, California Polytechnic State University, San Luis Obispo, CA 93407-0401, USA, [2]Department of Biology, University of North Carolina at Charlotte, Charlotte, NC 28223, USA and [3]Department of Oral Biology, University of Pittsburgh, Pittsburgh, PA 15261, USA

*Author for correspondence (ltomanek@calpoly.edu)

Accepted 23 February 2011

SUMMARY

Estuaries are characterized by extreme fluctuations in CO_2 levels due to bouts of CO_2 production by the resident biota that exceed its capacity of CO_2 consumption and/or the rates of gas exchange with the atmosphere and open ocean waters. Elevated partial pressures of CO_2 (P_{CO_2}; i.e. environmental hypercapnia) decrease the pH of estuarine waters and, ultimately, extracellular and intracellular pH levels of estuarine organisms such as mollusks that have limited capacity for pH regulation. We analyzed proteomic changes associated with exposure to elevated P_{CO_2} in the mantle tissue of eastern oysters (*Crassostrea virginica*) after 2 weeks of exposure to control (~39 Pa P_{CO_2}) and hypercapnic (~357 Pa P_{CO_2}) conditions using two-dimensional gel electrophoresis and tandem mass spectrometry. Exposure to high P_{CO_2} resulted in a significant proteome shift in the mantle tissue, with 12% of proteins (54 out of 456) differentially expressed under the high P_{CO_2} compared with control conditions. Of the 54 differentially expressed proteins, we were able to identify 17. Among the identified proteins, two main functional categories were upregulated in response to hypercapnia: those associated with the cytoskeleton (e.g. several actin isoforms) and those associated with oxidative stress (e.g. superoxide dismutase and several peroxiredoxins as well as the thioredoxin-related nucleoredoxin). This indicates that exposure to high P_{CO_2} (~357 Pa) induces oxidative stress and suggests that the cytoskeleton is a major target of oxidative stress. We discuss how elevated CO_2 levels may cause oxidative stress by increasing the production of reactive oxygen species (ROS) either indirectly by lowering organismal pH, which may enhance the Fenton reaction, and/or directly by CO_2 interacting with other ROS to form more free radicals. Although estuarine species are already exposed to higher and more variable levels of CO_2 than other marine species, climate change may further increase the extremes and thereby cause greater levels of oxidative stress.

Key words: cytoskeleton, estuary, hypercapnia, proteomics, oxidative stress, oyster.

INTRODUCTION

Estuarine ecosystems are among the most productive and biologically diverse areas of the ocean. However, estuarine zones are also characterized by high levels of environmental stress due to natural fluctuations in salinity, temperature, oxygen concentration and pH as well as anthropogenic pollution and nutrient input. Therefore, in order to survive in estuaries, organisms must possess efficient adaptive mechanisms that help them maintain homeostasis and provide stress protection in this highly variable environment.

Environmental pH is an important stressor in estuaries. Unlike the open ocean, where pH is relatively constant at approximately 8.2, the pH of estuarine waters may greatly fluctuate during the seasonal and diurnal cycles, from the values typical for the open ocean down to pH 7 or 6 (Hubertz and Cahoon, 1999; Ringwood and Keppler, 2002). Typically, bouts of low pH in estuarine waters coincide with the periods when carbon dioxide (CO_2) production due to respiration of the resident biota exceeds the capacity of CO_2 sinks (e.g. photosynthesis and dissipation to the atmosphere and/or open ocean waters). Additionally, freshwater influx and drainage from acidic soils may further decrease pH of estuarine waters (Lockwood, 1976; Perkins, 1974; Pritchard, 1967). In some estuaries, periods of low pH can persist for up to 4–5 months in summer and early fall (see long-term seasonal pH monitoring data at http://cdmo.baruch.sc.edu/), which may result in a considerable stress to the resident biota (Ringwood and Keppler, 2002). In future years, the global climate change driven by anthropogenically released CO_2 is predicted to lead to a significant acidification of the ocean waters (Caldeira and Wickett, 2003; Caldeira and Wickett, 2005), and this ocean acidification may further exacerbate the effects of seasonal and diurnal hypercapnia experienced by estuarine organisms. Currently, we do not have a full understanding of the potential stress effects of environmental hypercapnia and acidosis on estuarine organisms. An understanding of the physiological and molecular responses to hypercapnia in key estuarine organisms could therefore provide important new insights into the mechanisms of stress effects and factors that set limits to species' tolerance of elevated CO_2 and low pH in estuaries.

Recent progress in the application of proteomic methodologies has made it possible to identify a high percentage of proteins that change expression in response to shifting environmental conditions, even in non-model organisms with limited genomic information, e.g. by using expressed sequence tag (EST) libraries (for a review, see Tomanek, 2011). A number of proteomic studies on mollusks, specifically mussels, have provided insights into the molecular

mechanisms of stress response in these organisms, leading to the generation of new hypotheses and identifying new targets for physiological investigations. For example, proteomic studies on the sentinel genus *Mytilus* have demonstrated the importance of changes in post-translational modifications of proteins in response to pollution (Sheehan, 2007). A comparison of the proteomic changes in response to acute heat stress between two *Mytilus* congeners, *M. galloprovincialis* and *M. trossulus*, that differ in thermal tolerance (Braby and Somero, 2006) showed species-specific differences in the expression patterns of proteins involved in molecular chaperoning, protein degradation, cytoskeleton, energy metabolism, oxidative stress and lifespan, suggesting likely cellular pathways involved in evolution of thermal tolerance in these species (Tomanek and Zuzow, 2010). Thus, analysis of the global changes in the protein expression and identification of differentially expressed proteins is a fruitful avenue to obtain new knowledge about the potential molecular mechanisms of stress response in non-model organisms, such as marine mollusks.

Eastern oysters, *Crassostrea virginica*, are common bivalve mollusks that serve as ecosystem engineers in western Atlantic estuaries (Gutierrez et al., 2003). In the past century, populations of eastern oysters suffered severe declines due to overfishing, disease, water pollution and habitat destruction (Kirby, 2004), and restoration of oyster populations has been notoriously difficult (Schulte et al., 2009; Worm et al., 2009). The decrease in oyster populations led to dramatic changes in estuarine ecosystems that arguably went beyond the point of no return (Jackson, 2008; Jackson et al., 2001; Kirby, 2004). Environmental hypercapnia (i.e. elevated P_{CO_2} levels) and acidification of estuarine waters due to the increasing atmospheric CO_2 and eutrophication may pose an additional threat to oyster survival. However, currently the effects of environmental hypercapnia on oyster physiology are not well understood and require further investigation.

The goal of this study was to use the discovery approach of proteomics to identify the molecular responses of *C. virginica* to elevated CO_2 levels in seawater (environmental hypercapnia). We exposed oysters to control conditions (~39 Pa P_{CO_2}) and an elevated CO_2 concentration (~357 Pa P_{CO_2}) for 2 weeks, and used a quantitative proteomics approach based on the separation of proteins with two-dimensional (2-D) gel electrophoresis to detect changes in protein abundance, either due to *de novo* synthesis, post-translational modifications or degradation of proteins, in response to these conditions. Because this study focused on the potential molecular mechanisms of response to elevated CO_2, we selected a high P_{CO_2} level (~357 Pa) within the environmentally relevant range for oysters in order to elicit a clear cellular response. It is worth noting that such high P_{CO_2} levels are not uncommon in estuaries of the southeastern US where P_{CO_2} levels up to 1.3–4.7 kPa and pH levels of 7.5–6.0 are routinely recorded in summer (Cochran and Burnett, 1996; Ringwood and Keppler, 2002) (see also long-term water pH data for the eastern US estuaries at http://cdmo.baruch.sc.edu/). The duration of hypercapnic conditions in estuaries varies from hours to months. We chose a 2 week time period because it is in the middle of the exposure time scales. Using a database of ESTs and tandem mass spectrometry, we identified two categories of proteins – those associated with the cytoskeleton and those associated with oxidative stress – that changed abundance in response to the high CO_2 level. To our knowledge, there is no other study to date using proteomics to assess the cellular effects of environmental hypercapnia in marine organisms that provides insights into the potential mechanisms involved in stress response to and tolerance of high CO_2 levels.

MATERIALS AND METHODS

Animal maintenance and experimental exposures

Adult *Crassostrea virginica* Gmelin 1791 (approximately 2 years old, 8–12 cm shell length) were obtained from a commercial supplier (Taylor Shellfish Farms, Shelton, WA, USA) and acclimated for 1 week at 20°C and 30‰ salinity in recirculating water tanks with artificial seawater (ASW; Instant Ocean®, Pet Solutions, Beavercreek, OH, USA) prior to experimentation. During this preliminary acclimation, tanks were aerated with ambient air.

After the preliminary acclimation, oysters were divided into eight batches (five adults per batch) and each batch was randomly assigned to either the elevated P_{CO_2} (357 Pa P_{CO_2} or pH 7.5) or control treatment (39 Pa P_{CO_2} or pH 8.3). For each treatment, four replicate tanks (20°C and 30‰ salinity) were set up, each containing five oysters at a density of 1 oyster l^{-1} ASW. For elevated P_{CO_2} treatments (environmental hypercapnia), ASW was vigorously bubbled with commercial gas mixtures containing 0.5% CO_2, 21% O_2 and balance nitrogen obtained from Roberts Oxygen (Charlotte, NC, USA). The gas content of the mixtures was analyzed by the manufacturer and certified to be accurate within 10% of the target value. The control (normocapnic) treatments were bubbled with ambient air. In both cases, gas flow through the seawater was adjusted in such a way that further increases in flow rate did not result in a change in pH, indicating that experimental systems were at steady-state with respect to gas saturation. Water was changed every other day using ASW pre-bubbled with air or CO_2-enriched gas mixture as appropriate. Oxygen levels in experimental tanks ranged between 100 and 97% of air saturation throughout all exposures as measured with Clark-type oxygen probes (YSI 5300A biological oxygen monitor with YSI 5331 oxygen probe, YSI Incorporated, Yellow Springs, OH, USA).

For water chemistry analyses, seawater samples were collected in air-tight 50 ml containers without air space to prevent gas exchange with the atmosphere, stabilized by mercuric chloride poisoning (Dickson et al., 2007) and immediately shipped to Nutrient Analytical Services (Chesapeake Biological Laboratory, Solomons, MD, USA) for analysis. Samples were kept in the dark at +4°C during shipping and storage, and analyzed within 1 week of collection. Total dissolved inorganic carbon (DIC) concentrations were measured with Shimadzu TOC5000 gas analyzer equipped with an infrared NDIR CO_2 detector (Shimadzu Scientific Instruments, Columbia, MD, USA). Ambient barometric pressure, temperature, salinity and pH were measured for each sample at the time of sample collection and, along with the total DIC levels, were used to calculate P_{CO_2} and alkalinity in seawater using co2sys software (Lewis and Wallace, 1998). Water pH was measured using a pH electrode (pH meter Model 1671, Jenco Instruments, San Diego, CA, USA) calibrated with National Institute of Standards and Technology (NIST) standard pH solutions. For co2sys settings, we used the NBS scale of seawater pH, constants from Millero et al. (Millero et al., 2006) and the KSO_4 constant from Dickson et al. (Dickson et al., 1990) (Lewis and Wallace, 1998), and concentrations of silicate and phosphate for ASW of 0.17 and 0.04 μmol kg^{-1}, respectively, at 30‰. These experimental exposures were identical to those reported in a previous study (Beniash et al., 2010), and a summary of the relevant water chemistry parameters is given in Table 1.

During the preliminary acclimation and experimental incubations, oysters were fed every other day immediately following the water change with a commercial algal blend *ad libitum* (5 ml per tank) containing *Nannochloropsis oculata*, *Phaeodactylum tricornutum* and *Chlorella* sp. with a cell size of 2–20 μm (DT's Live Marine

Table 1. Summary of the water chemistry parameters during experimental exposures

Parameter	Control	High CO_2 exposure
Salinity (‰)	30.1±0.2	30.0±0.1^{ns}
Temperature (°C)	20.0±0.1	20.0±0.1^{ns}
pH (NBS scale)	8.3±0.1	7.5±0.0**
DIC (mmol kg^{-1} SW)	2899.4±364.9	3384.8±245.7**
P_{CO_2} (Pa)	39.05±2.27	357.00±22.49***
Total alkalinity (mmol kg^{-1} SW)	3320.1±454.0	3341.8±242.9^{ns}

Salinity, temperature, pH and dissolved inorganic carbon (DIC) were measured in samples from experimental tanks, and P_{CO_2} and total alkalinity were calculated using co2sys software (Beniash et al., 2010; Lewis and Wallace, 1998).

Data are presented as means ± s.d.; N=7 for control exposures, N=14 for high CO_2 exposures.

Differences between the control and high CO_2 conditions were tested using GLM ANOVA. ns, differences not significant (P>0.05); **, P<0.01; ***, P<0.001.

SW, sea water.

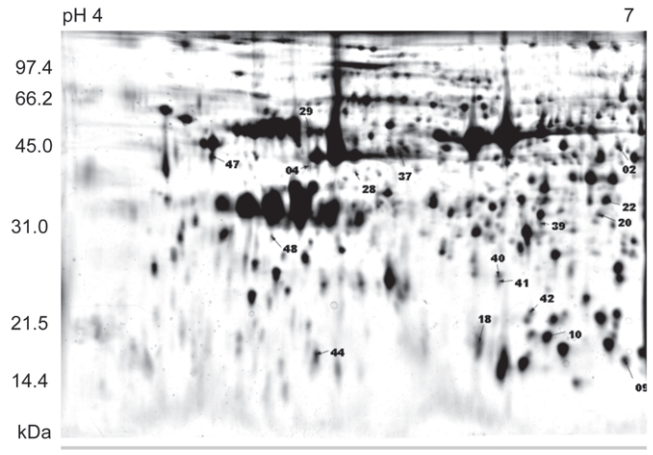

Fig. 1. A composite gel image (or proteome map) of twenty 2-D gel images of eastern oyster (*Crassostrea virginica*) mantle tissue exposed to normal and elevated CO_2 levels for 2 weeks. The image represents the mean pixel volume for each of the 456 detected protein spots. The numbers correspond to proteins that significantly changed in abundance in response to treatment conditions and identified by tandem mass spectrometry (for identifications see Table 2).

Phytoplankton, Sycamore, IL, USA). No mortality of oysters was detected throughout the experiment.

Tissue homogenization

Mantle tissue was thawed and homogenized with a chilled ground-glass homogenizer using a ratio of 1:4 of tissue to ice-cold buffer containing 7 mol l^{-1} urea, 2 mol l^{-1} thiourea, 23 mmol l^{-1} ASB-14 (amidosulfobetaine-14), 40 mmol l^{-1} Tris-base, 0.5% immobilized pH 4–7 gradient (IPG) buffer (GE Healthcare, Piscataway, NJ, USA) and 40 mmol l^{-1} dithiothreitol. Following centrifugation at room temperature for 30 min at 16,100 ***g***, the supernatant was precipitated by adding four volumes of ice-cold 10% trichloroacetic acid in acetone and stored at –20°C overnight. The next day the precipitated proteins were collected by centrifugation at 4°C for 15 min at 18,000 ***g***, the supernatant was discarded and the remaining pellet was washed with ice-cold acetone and centrifuged again. The washed pellet was quickly resuspended by vortexing (5 min) in rehydration buffer [7 mol l^{-1} urea, 2 mol l^{-1} thiourea, 3.25 mmol l^{-1} cholamidopropyl-dimethylammonio-propanesulfonic acid (CHAPS), 2% nonyl phenoxylpolyethoxylethanol-40 (NP-40), 0.0005% Bromophenol Blue, 0.5% IPG buffer, 100 mmol l^{-1} dithioerythritol]. The protein concentration was determined with the 2D Quant kit (GE Healthcare, Piscataway, NJ, USA), according to the manufacturer's instructions.

Two-dimensional gel electrophoresis

Proteins were separated according to their isoelectric point (pI) on immobilized pH gradient (IPG) strips (pH 4–7, 11 cm; GE Healthcare) using 400 µg of protein per strip. The isoelectric focusing protocol started with a passive rehydration step (5 h), followed by 12 h of active rehydration (50 V) using an isoelectric focusing cell (BioRad, Hercules, CA, USA). The following running conditions were used during the isoelectric focusing run: 500 V for 1 h, 1000 V for 1 h and 8000 V for 2.5 h (all changes occurred in rapid mode). Following isoelectric focusing, gel strips were frozen at –80°C.

To run the second gel dimension (separation of proteins by molecular mass), the frozen IPG strips were thawed and incubated in equilibration buffer [375 mmol l^{-1} Tris-base, 6 mol l^{-1} urea, 30% glycerol, 2% sodium dodecyl sulfate (SDS), 0.0002% Bromophenol Blue] for 15 min, first with 65 mmol l^{-1} dithiothreitol and then, after decanting the solution, with 135 mmol l^{-1} iodoacetamide in equilibration buffer. IPG strips were placed on top of an 11.8% polyacrylamide gel with a 0.8% agarose solution containing Laemmli SDS electrophoresis buffer (25 mmol l^{-1} Tris-base, 192 mmol l^{-1} glycine, 0.1% SDS). The vertical slab gels were run at 200 V for 55 min with a recirculating water bath set at 10°C using Criterion Dodeca cells (BioRad). Gels were stained with colloidal Coomassie Blue dye (G-250) overnight and destained by washing repeatedly with Milli-Q water for at least 48 h. The resulting 2-D gel images were scanned with an Epson 1280 transparency scanner (Epson, Long Beach, CA, USA).

Gel image analysis

Digitized images of 2-D gels were analyzed with Delta2D image software (version 3.6; Decodon, Greifswald, Germany) (Berth et al., 2007). The gels were compared with each other using the group warping strategy by creating match vectors between the gels within a treatment group and then the first gels between each treatment. All 20 images were fused into a composite image (=proteome map), which represents mean volumes for each protein spot (Fig. 1). The proteome map was used to detect spot boundaries, which were subsequently transferred back to all 20 gel images using the previously generated match vectors. After background subtraction, protein spot volumes were normalized against total spot volume of all protein spots of a gel image.

Mass spectrometry

Following the statistical analysis, proteins that significantly changed in abundance in response to elevated P_{CO_2} conditions were excised from representative gels using a tissue puncher (Beecher Instruments, Prairie, WI, USA). The excised gel plugs were destained by two washes with 25 mmol l^{-1} ammonium bicarbonate in 50% acetonitrile before dehydration with 100% acetonitrile and subsequent digestion with 11 ng µl^{-1} trypsin (Promega, Madison, WI, USA) overnight at 37°C. We used elution buffer [0.1% trifluoroacetic acid (TFA): acetonitrile 2:1] and a SpeedVac (Thermo

Fisher Scientific, Waltham, MA, USA) to extract and concentrate digested proteins. The digested proteins in elution buffer were mixed with 5 µl of matrix solution (0.2 mg ml^{-1} a-hydroxycyano cinnamic acid in acetonitrile) and spotted on an Anchorchip® target plate (Bruker Daltonics Inc., Billerica, MA, USA). Proteins spotted to the target were washed with 0.1% TFA in 10 mmol l^{-1} ammoniumphosphate and re-crystallized using an acetone:ethanol:0.1% TFA (6:3:1 v:v:v) mixture.

Peptide mass fingerprints (PMFs) were obtained on a matrix-assisted laser desorption ionization tandem time-of-flight (MALDI-TOF-TOF) mass spectrometer (Ultraflex II; Bruker Daltonics Inc.). Following PMFs, we selected six or more peptides from the spectrum for further fragmentation through tandem mass spectrometry. The resulting spectra contained information about the peptides' b- and y-ions, specific fragment types that can be used to decipher the peptide's amino acid sequence. However, given a putative match they can also be compared with the theoretical b- and y-ions. We used the latter approach to confirm protein identity by finding at least two peptides whose fragments matched the theoretical ones from the putative match that we obtained after conducting the PMF alone.

Mass spectra were analyzed with flexAnalysis (version 3.0; Bruker Daltonics Inc.) by applying the following conditions: TopHat algorithm for baseline subtraction, Savitzky-Golay analysis for smoothing (0.2 *m/z*; number of cycles=1) and SNAP algorithm for peak detection (signal-to-noise ratio: 6 for MS and 1.5 for MS/MS). The charge state of the peptides was assumed to be +1. Porcine trypsin was used for internal mass calibration.

Proteins were identified using Mascot (version 2.2; Matrix Science Inc., Boston, MA, USA) by combining PMFs and tandem mass spectra in a search against a database. The database we used contained approximately 44,390 oyster-specific ESTs and was constructed from the NCBI taxonomy browser (http://www.ncbi.nlm.nih.gov/Taxonomy/). We used the following search parameters: we chose oxidation of methionine and carbamidomethylation of cysteine as variable modifications, and allowed for one missed cleavage during trypsin digestion. For tandem mass spectrometry, we set the precursor-ion mass tolerance to 0.6 Da. Specifically, given our database, individual molecular weight search (MOWSE) ion scores greater than 41 indicated significant identity (P<0.05). Our search results that were obtained with the oyster EST database were tested against a decoy database (using Mascot) and resulted in no detection of false positives. However, we only accepted positive identifications that included two matched peptides regardless of the MOWSE score (Table 2).

Statistical analysis

Normalized spot volumes were analyzed within Delta2D using a *t*-test based on a null distribution that was generated using 1000 permutations of the data, thus accounting for any non-normal distribution and unequal variance of the response variables (protein spot volumes). For the *t*-test, we used a *P*-value of 0.02 to limit the number of false positives to account for the multiple comparisons instead of using a slightly more conservative false-discovery approach while maintaining the customary *P*-value of 0.05. For the hierarchical clustering, we used average linking within the statistical tool suite in Delta2D using Pearson's correlation coefficients.

RESULTS

A proteome map representing the mean pixel volume of all proteins detected in the 20 analyzed mantle tissue samples is shown in Fig. 1. Overall, we detected a total of 456 individual protein spots after evaluating spot boundaries. Following a *t*-test based on permutations, we found 54 (or 12%) of the total number of spots that significantly changed abundance in response to elevated P_{CO_2} (P<0.02). Of those 54, we were able to identify 17 proteins (or 31%, labeled by number in Fig. 1 and listed in Table 2); this number is below the percentage of proteins that have been identified in other non-model mollusks in an earlier study (Tomanek and Zuzow, 2010). Hierarchical clustering shows that the expression patterns of the 17 identified proteins separate into two major clusters: a smaller cluster with three proteins (peroxiredoxin 2, collagen, and Rab1b precursor) characterized by downregulation under elevated P_{CO_2} conditions, and a larger cluster of 14 proteins characterized by upregulation under high P_{CO_2} conditions (Fig. 2).

The functions of the majority of identified proteins (82%) fall into two main categories: those that comprise part of the cytoskeleton, including elements of the G-protein signaling processes that affect the cytoskeleton, and those involved in an oxidative stress response (Fig. 4). Three proteins have other functions related to energy and/or protein metabolism (Fig. 4). Among the cytoskeleton-related proteins, expression of actin, actin-polymerization factor and calponin 2 was significantly elevated in the mantle tissue of oysters exposed to high P_{CO_2} for 2 weeks (P<0.02; Fig. 3) whereas collagen (type XII) expression decreased (Fig. 3). Two identified signaling proteins showed different patterns of change in response to 2 weeks exposure to high P_{CO_2}: Rap1b protein expression was downregulated and the receptor of activated protein kinase C was upregulated under elevated P_{CO_2} conditions (P<0.02; Fig. 3). Notably, the majority of the identified antioxidant proteins were significantly upregulated under high P_{CO_2} conditions, including peroxiredoxins 2, 4 and 5, nucleoredoxin and cytosolic *Cu,Zn*-superoxide dismutase (SOD) (Fig. 4). Exposure to high CO_2 levels also resulted in upregulation of mitochondrial malate dehydrogenase, an important Krebs cycle enzyme, and 40S ribosomal protein and proteasome α type 3 protein, which are involved in protein synthesis and degradation (Fig. 4).

DISCUSSION

A proteomics approach is an excellent tool to provide insights into hitherto unknown responses to environmental stress, such as elevated P_{CO_2}, at the level of the molecular phenotype, by quantifying changes in the global protein expression that reflect changes in protein synthesis, post-translational modifications or degradation (Tomanek, 2011). To our knowledge, to date there is no other study reporting on the proteomic changes in response to elevated P_{CO_2} in any marine organism. Our study showed a significant shift in the proteome of the mantle tissue of oysters *C. virginica* exposed to elevated P_{CO_2} levels and reduced pH (~357 Pa, pH ~7.5) that are within the environmentally relevant range for this species. Indeed, in many southeastern US estuaries, pH and P_{CO_2} levels can fluctuate from the values close to those of the open ocean (pH ~8.0, ~40 Pa P_{CO_2}) during the cold season to pH values as low as 6.0 and P_{CO_2} levels as high as 1.3–4.7 kPa in summer on a time scale from hours to months (Cochran and Burnett, 1996; Burnett, 1997; Hubertz and Cahoon, 1999; Ringwood and Keppler, 2002) (see also long-term seasonal pH monitoring data at http://cdmo.baruch.sc.edu/). Interestingly, although the elevated P_{CO_2} level used in the present study (~357 Pa) represents a relatively modest hypercapnia by estuarine standards, it nevertheless causes a considerable change in cellular phenotype of oysters. Indeed, approximately 12% of all proteins in the mantle tissue changed their abundance in response to the elevated P_{CO_2} of ~357 Pa. Despite the limited genomic information available for eastern oysters, we were able to identify

Table 2. Protein identifications and fold changes with hypercapnia treatment in mantle tissue of the eastern oyster, *Crassostrea virginica*

Spot ID	Protein ID	M_r (kDa) estimated	pI estimated	M_r (kDa) predicted	pI predicted	GenBank ID	MOWSE score	Peptide matches	Sequence coverage (%)	Mean normalized volume 39 Pa P_{CO_2}	Mean normalized volume 357 Pa P_{CO_2}	Ratio	Functional category
2	Calponin 2	52.00	6.90	33.80	6.60	gil164568905	47	2	4	0.129± 0.007	0.168± 0.011	1.305	Cytoskeleton
4	Actin	47.00	5.30	41.80	5.30	gil32423714	74	2	7	0.107± 0.016	0.181± 0.012	1.688	Cytoskeleton
9	Actin depolymerization factor-1 (ADF)	11.00	6.90	17.30	7.60	gil31904714	51	2	13	0.163± 0.011	0.252± 0.016	1.546	Cytoskeleton
10	Peroxiredoxin-5	14.00	6.50	19.60	8.30	gil152818317	141	4	32	0.365± 0.006	0.453± 0.024	1.241	Oxidative stress
18	*Cu,Zn*-superoxide dismutase	14.00	6.10	16.00	6.10	gil22598381	114	2	6	0.214± 0.015	0.329± 0.017	1.539	Oxidative stress
20	Receptor of activated kinase C	35.00	6.80	35.00	7.00	gil31906094	115	4	23	0.084± 0.005	0.111± 0.007	1.315	Cell signaling
22	Mitochondrial malate dehydrogenase (mMDH)	37.00	6.80	35.00	8.40	gil152813302	105	3	13	0.239± 0.009	0.314± 0.016	1.315	Energy metabolism
28	Actin	45.00	5.50	41.70	5.30	gil31905164	44	2	9	0.021± 0.003	0.050± 0.005	2.298	Cytoskeleton
29	Collagen type 6, α6	57.00	5.30	25.50	6.80	gil84142151	64	2	11	0.595± 0.032	0.412± 0.027	0.694	Extracellular matrix
37	Actin	50.00	5.80	41.80	5.30	gil22598136	51	2	12	0.112± 0.033	0.260± 0.045	2.321	Cytoskeleton
39	Thioredoxin peroxidase	32.00	6.50	25.00	8.40	gil13488586	82	2	11	0.066± 0.004	0.116± 0.010	1.751	Oxidative stress
40	Peroxiredoxin 2	23.00	6.30	22.30	7.60	gil164571416	240	4	23	0.082± 0.008	0.049± 0.005	0.601	Oxidative stress
41	Peroxiredoxin 2	23.00	6.25	22.30	7.60	gil164571416	240	4	23	0.033± 0.005	0.093± 0.009	2.778	Oxidative stress
42	Rap-1b precursor	17.00	6.40	20.80	6.40	gil189407780	134	2	4	0.086± 0.005	0.042± 0.007	0.490	Cell signaling
44	Nucleoredoxin	12.00	5.30	45.20	9.40	gil14580680	143	5	18	0.166± 0.016	0.293± 0.040	1.770	Oxidative stress
47	40S ribosomal protein SA	50.00	4.80	33.50	5.20	gil31900908	235	4	15	0.127± 0.015	0.180± 0.010	1.417	Cell adhesion
48	Proteasome β type 3	30.00	5.00	23.00	5.40	gil164584631	117	3	18	0.024± 0.004	0.097± 0.015	4.013	Protein degradation

Relative molecular masses (M_r) and isoelectric points (pI) are estimated according to the spots' position on the proteome map (Fig. 1). Ratios of hypercapnia/normcapnia are the mean levels of expression (abundance) under hypercapnic treatment relative to the normcapnia control treatment [values <1.0 (>1.0) indicate a decrease (increase) in protein abundance].
Mean volumes are presented ±s.e.m.

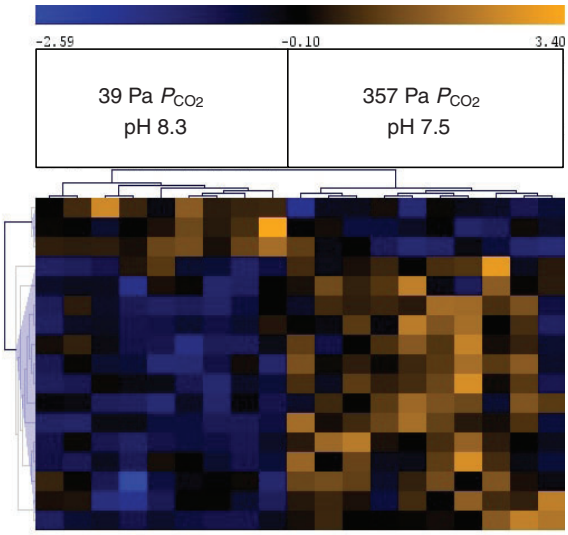

Fig. 2. Hierarchical clustering of identified proteins using Pearson's correlation coefficient in control and elevated P_{CO_2} conditions in mantle tissue of the eastern oyster (*Crassostrea virginica*). Blue, lower than average standardized volume; orange, higher than average standardized volume. The horizontal axis represents the standardized (spot volume against total volume) volume of the respective protein relative to its average volume within each treatment; the vertical axis represents the standardized volumes of those proteins that belong to one particular gel.

17 differentially expressed proteins – 31% of which significantly changed their expression patterns under elevated P_{CO_2} conditions.

The majority of proteins differentially expressed under control and elevated P_{CO_2} conditions fall into two functional categories: those associated with the cytoskeleton, including collagen, actin, actin depolymerization factor and calponin, and those involved in antioxidant defense, including superoxide dismutase and several peroxiredoxins (Figs 3 and 4). Notably, five of the six antioxidant proteins were upregulated in response to elevated P_{CO_2}, indicating pro-oxidant conditions and potential oxidative stress in the cells (Fig. 4). Among these, peroxiredoxins occupy a prominent place, a group of cellular antioxidants involved in the detoxification of organic peroxides and hydrogen peroxide (Ishii and Yanagawa, 2007). Two peroxiredoxins that were upregulated under the conditions of elevated P_{CO_2} are peroxiredoxin 4, located in the endoplasmic reticulum, and peroxiredoxin 5, found throughout the cell, including in the cytosol and mitochondria (Cox et al., 2010). The cytosolic

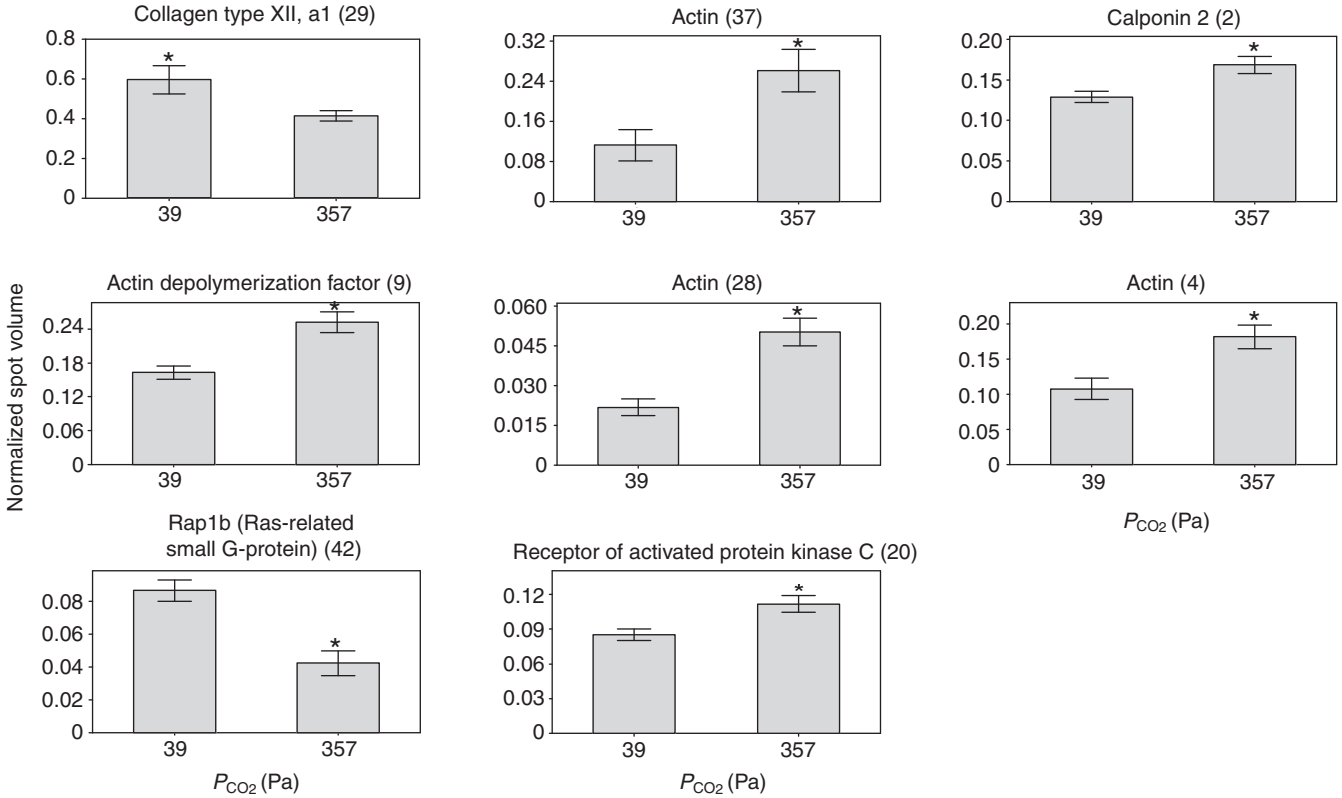

Fig. 3. Abundance levels of cytoskeleton-associated and signaling proteins identified in mantle tissue of the eastern oyster (*Crassostrea virginica*) exposed to control (~39 Pa) and elevated (~357 Pa) P_{CO_2}. Protein spot volumes were obtained by normalizing against the total volume of all protein spots and are means ± 1 s.e.m. (N=10). The number of the corresponding spot on the proteome map (Fig. 1) is given in brackets. Asterisks indicate a significant difference (P<0.02) based on a t-test (see text for details). Different graphs for actin refer to different spots on the proteome map that were identified as the same protein, representing either a splice isoform, a paralogous homolog or a position shift due to post-translational modification.

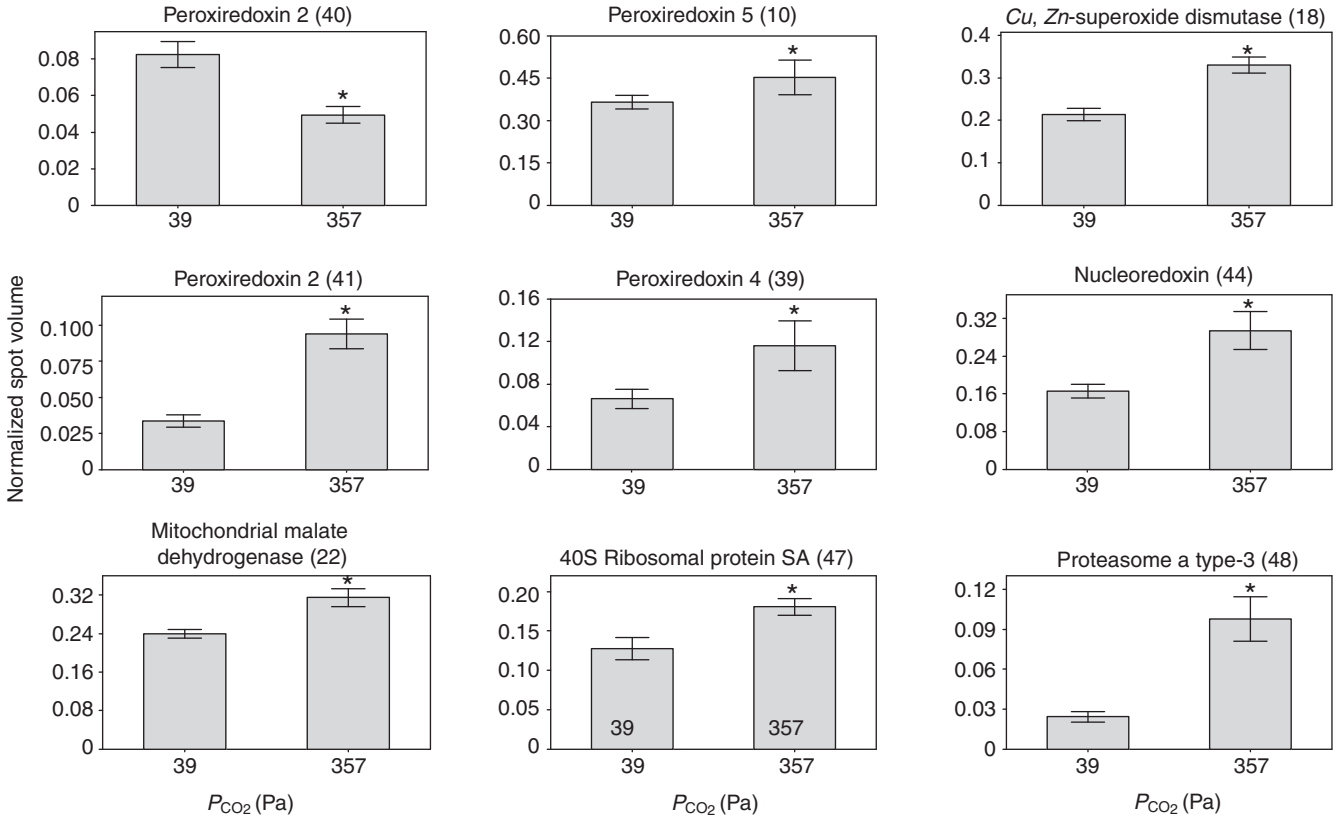

Fig. 4. Abundance levels of antioxidant proteins and proteins involved in energy and protein metabolism identified in mantle tissue of the eastern oyster (*Crassostrea virginica*) exposed to control (~39 Pa) and elevated (~357 Pa) P_{CO_2}. Protein spot volumes were obtained by normalizing against the total volume of all protein spots and are means ± 1 s.e.m. (N=10). The number of the corresponding spot on the proteome map (Fig. 1) is given in brackets. Asterisks indicate a significant difference (P<0.02) based on a t-test (see text for detail). Different graphs for peroxiredoxin 2 refer to different spots on the proteome map that were identified as the same protein, likely reflecting a position shift due to post-translational modification.

peroxiredoxin 2, the only oxidative stress protein that was downregulated under high P_{CO_2} conditions, was also identified as being upregulated in a nearby spot (spot 41 *versus* 40; Fig. 1) in response to elevated P_{CO_2}, suggesting that a post-translational modification (Barranco-Medina et al., 2009) or a C-terminal truncation (Koo et al., 2002) induced a shift in the protein position on the proteome map. In addition to the thioredoxin-related proteins, cytosolic *Cu*,*Zn*-SOD, an enzyme that catalyzes the dismutation of superoxide anion ($O_2^{\cdot}$) to hydrogen peroxide (H_2O_2), is also upregulated under elevated P_{CO_2} conditions. Superoxide is mainly produced by the electron transport chain in the mitochondria but can also be generated by cytosolic, peroxisomal and membrane enzymes including monooxygenases and NADPH-dependent oxidases (Halliwell and Gutteridge, 1999; Mohazzab et al., 1994; Murphy, 2009). Although mitochondria are the major site of ROS production in the cell, peroxisomes and high NADPH-oxidase activity can substantially contribute to the formation of ROS in some cell types, such as phagocytic hemocytes found in oyster mantle tissue (Boyd and Burnett, 1999; Fang, 2004; Go and Jones, 2008). Upregulation of cytosolic antioxidants such as peroxiredoxins and *Cu*,*Zn*-SOD suggests that elevated P_{CO_2} induces oxidative stress in the cytosol of the mantle cells of oysters. Interestingly, exposure to elevated P_{CO_2} also induces elevated expression of nucleoredoxin, a protein related to the thioredoxin family (Funato and Miki, 2007), members of which reduce oxidized peroxiredoxin (Cox et al., 2010; Meyer et al., 2009). Although the function of nucleoredoxin is not yet fully understood, this protein was shown to regulate cell fate and early development in a redox-dependent manner (Funato and Miki, 2007), so that its upregulation in the mantle cells of oysters exposed to elevated P_{CO_2} is consistent with the putative shift of the cellular redox status towards oxidative stress.

The finding of upregulated antioxidant defense systems in oysters exposed to elevated P_{CO_2} is novel and begs further investigation into the mechanisms that can lead to elevated oxidative stress under these conditions. There are at least three possible non-mutually exclusive hypotheses that can explain how increased levels of CO_2 can cause oxidative stress. One possible route is that CO_2 directly affects ROS production by reacting with peroxynitrite ($ONOO^-$), a very reactive nitrogen species that is formed through the reaction between superoxide anions and nitric oxide (Dean, 2010). This spontaneous reaction results in formation of reactive carbonate, oxygen and nitrogen species that can oxidize multiple cellular compounds including thiols, aromatic compounds, cytochromes and other heme-containing molecules, thus resulting in oxidative stress (Denicola et al., 1996; Meli et al., 2002). Future studies are required to measure intracellular concentrations of CO_2, bicarbonate and peroxynitrite achieved in control and high P_{CO_2} treatments in order to determine whether this reaction can also occur under the *in vivo* conditions in oyster cells. Alternatively, a possible explanation for elevated oxidative stress under high P_{CO_2} conditions is the indirect effects of elevated CO_2 and/or low pH on mitochondrial function and/or non-enzymatic production of free radicals. Mollusks including oysters have a limited capability for pH regulation so that

acidification of seawater results in extracellular and intracellular acidosis (Burnett, 1997). Low intracellular pH triggered by environmental acidification may negatively affect the efficiency of the mitochondrial electron transport chain (ETC) by increasing electron slip in ROS-generating mitochondrial complexes I and III and/or by partially inhibiting the flow through the downstream ETC complexes (Murphy, 2009; Starkov, 2006). In either case, these disturbances of the ETC function would result in elevated rates of ROS generation. Intracellular acidosis can also lead to the release of chelated transition metals such as Fe^{2+} from intracellular stores (Dean, 2010). Excess of free intracellular iron induces oxidative stress by catalyzing Fenton reactions and generating hydroxyl radicals (Stohs and Bagchi, 1995). In mammalian cells, intracellular acidosis leads to elevated oxidative injury that can be prevented by iron chelators, indicating a key role of iron release in the acid-induced oxidative damage (Ballard and Dean, 2001; Bronk and Gores, 1991; Levraut et al., 2003). Interestingly, metabolic acidosis during anoxic exposure also led to an upregulation of an iron-chelating protein, ferritin, in a marine snail *Littorina littorea* (English and Storey, 2003), suggesting that iron release may also be triggered by intracellular acidosis in mollusks. All the above-discussed mechanisms of pH- and CO_2-induced oxidative damage have been demonstrated mostly in mammalian models; therefore, their putative involvement in oxidative stress of mollusks exposed to environmental hypercapnia remains to be investigated. It is worth noting that hypercapnic conditions are typically accompanied by hypoxic conditions in estuaries and that hypoxic conditions also generate ROS (Murphy, 2009). However, the molecular mechanisms causing increased ROS production under reduced oxygen conditions are not well understood, especially in non-model organisms such as oysters, and require further investigation (reviewed in Aragones et al., 2009; Clanton, 2007; Murphy, 2009). We plan follow-up studies investigating the effects of hypercapnia under hypoxia to compare the proteomic responses under both conditions and assess possible common pathways.

One intriguing finding of the present study is the concomitant upregulation of antioxidant and cytoskeletal proteins. A plausible explanation for the co-expression of these two functional groups is that the cytoskeleton is a major target of ROS and reactive nitrogen species (Dalle-Donne et al., 2001; Tell, 2006). Under conditions of oxidative stress, ROS-sensitive cysteine residues of actin either form intermolecular disulfide bridges or undergo reversible S-glutathionylation, which may confer protection against ROS (Dalle-Donne et al., 2003a; Dalle-Donne et al., 2003b). The changing abundances of three actin spots could thus represent either increased expression or post-translational modifications of these forms of actin. Such changes in cytoskeleton may be triggered by Rap1, a small G-protein of the Ras family, implicated in affecting a number of proteins that modify the actin-based cytoskeleton (Bos, 2005; Pannekoek et al., 2009).

In addition to oxidative stress and changes in the expression of cytoskeleton-related proteins, elevated P_{CO_2} also resulted in upregulation of mitochondrial malate dehydrogenase, a ribosomal protein and a proteasome subunit (Figs 3 and 4), indicating possible effects of elevated P_{CO_2} and/or reduced pH on energy metabolism, protein synthesis and degradation in oysters (Glickman and Ciechanover, 2002; Kossinova et al., 2008) and was suggested by earlier studies (Beniash et al., 2010; Lannig et al., 2010; Michaelidis et al., 2005; Rosa and Seibel, 2008) (but see Gutowska et al., 2008).

Perspectives and significance

Although the present study of proteomic responses to elevated P_{CO_2} in oysters is limited to a 2 week exposure, it offers insights into the possible stress and adaptive responses of sessile estuarine organisms to hypercapnic conditions that naturally occur in estuaries (Burnett, 1997; Cochran and Burnett, 1996). This study also demonstrates the value of a discovery-oriented proteomic approach in identifying new cellular and physiological pathways that are likely to be involved in adaptive response to high CO_2 and/or low pH stress, such as regulation of antioxidants and the cytoskeleton. Regardless of the exact molecular mechanisms responsible for cellular redox shifts in oysters exposed to elevated P_{CO_2} levels, these shifts are likely to represent an energy liability for organisms requiring additional investment in cellular defense and protection systems (as indicated by upregulation of antioxidants), and possibly damage repair to the cytoskeleton.

Although the experimental conditions in our study are environmentally relevant to the present and the immediate future of estuaries, the P_{CO_2} levels used are two to three times higher than the levels predicted for the atmosphere and the open ocean under future climate scenarios (IPCC, 2007). Nevertheless, demonstration of the considerable shifts in the molecular phenotype of oyster cells in response to hypercapnia may complement recent studies on the effects of ocean acidification at the whole-organism level in marine animals (Doney et al., 2009; Pörtner et al., 2004) and inform future studies looking into physiological and cellular mechanisms of the effects of ocean acidification using moderate P_{CO_2} conditions. Specifically, it is important to determine whether lower CO_2 levels predicted for the open ocean conditions of the near future can also elicit oxidative stress and cytoskeletal changes in oyster mantle, and whether these changes in cellular phenotype are linked to a decrease in biomineralization at elevated P_{CO_2} that has been documented for oysters and other bivalves (Michaelidis et al., 2005; Miller et al., 2009; Ries et al., 2009) and/or to changes in other physiological functions (such as energy metabolism) that can affect an organism's fitness.

ACKNOWLEDGEMENTS

We thank Dr Jennifer Oquendo for several helpful editorial suggestions. L.T. was supported by the National Science Foundation award IOS-0717087 during the course of this study. This work was in part supported by funds provided by the National Science Foundation award IOS-0951079 and North Carolina Sea Grant Minigrant (R/MG-0906) to I.M.S. and E.B., and a UNC Charlotte Faculty Research Grant to I.M.S.

REFERENCES

Aragones, J., Fraisl, P., Baes, M. and Carmeliet, P. (2009). Oxygen sensors at the crossroad of metabolism. *Cell Metab.* **9**, 11-22.
Ballard, J. W. O. and Dean, M. D. (2001). The mitochondrial genome: mutation, selection and recombination. *Genomes Evol.* **11**, 667-672.
Barranco-Medina, S., Lazaro, J. J. and Dietz, K. J. (2009). The oligomeric conformation of peroxiredoxins links redox state to function. *FEBS Lett.* **583**, 1809-1816.
Beniash, E., Ivanina, A., Lieb, N. S., Kurochkin, I. and Sokolova, I. (2010). Elevated level of carbon dioxide affect metabolism and shell formation in oysters *Crassostrea virginica* (Gmelin). *Mar. Ecol. Prog. Ser.* **419**, 95-108.
Berth, M., Moser, F. M., Kolbe, M. and Bernhardt, J. (2007). The state of the art in the analysis of two-dimensional gel electrophoresis images. *Appl. Microbiol. Biotechnol.* **76**, 1223-1243.
Bos, J. L. (2005). Linking Rap to cell adhesion. *Curr. Opin. Cell Biol.* **17**, 123-128.
Boyd, J. N. and Burnett, L. E. (1999). Reactive oxygen intermediate production by oyster hemocytes exposed to hypoxia. *J. Exp. Biol.* **202**, 3135-3143.
Braby, C. E. and Somero, G. N. (2006). Following the heart: temperature and salinity effects on heart rate in native and invasive species of the blue mussels (genus *Mytilus*). *J. Exp. Biol.* **209**, 2554-2566.
Bronk, S. F. and Gores, G. J. (1991). Acidosis protects against lethal oxidative injury of liver sinusoidal endothelial cells. *Hepatology* **14**, 150-157.
Burnett, L. E. (1997). The challenges of living in hypoxic and hypercpnic aquatic environments. *Am. Zool.* **37**, 633-640.
Caldeira, K. and Wickett, M. E. (2003). Oceanography: anthropogenic carbon and ocean pH. *Nature* **425**, 365.

Caldeira, K. and Wickett, M. E. (2005). Ocean model predictions of chemistry changes from carbon dioxide emissions to the atmosphere and ocean. *J. Geophys. Res Oceans* **110**.
Clanton, T. L. (2007). Hypoxia-induced reactive oxygen species formation in skeletal muscle. *J. Appl. Physiol.* **102**, 2379-2388.
Cochran, R. E. and Burnett, L. E. (1996). Respiratory responses of the salt marsh animals, *Fundulus heteroclitus*, *Leiostomus xanthurus*, and *Palaemonetes pugio* to environmental hypoxia and hypercapnia and to the organophosphate pesticide, azinphosmethyl. *J. Exp. Mar. Biol. Ecol.* **195**, 125-144.
Cox, A. G., Winterbourn, C. C. and Hampton, M. B. (2010). Mitochondrial peroxiredoxin involvement in antioxidant defence and redox signaling. *Biochem. J.* **425**, 313-325.
Dalle-Donne, I., Rossi, R., Milzani, A., Di Simplicio, P. and Colombo, R. (2001). The actin cytoskeleton response to oxidants: from small heat shock protein phosphorylation to changes in the redox state of actin itself. *Free Radic. Biol. Med.* **31**, 1624-1632.
Dalle-Donne, I., Giustarini, D., Rossi, R., Colombo, R. and Milzani, A. (2003a). Reversible S-glutathionylation of Cys 374 regulates actin filament formation by inducing structural changes in the actin molecule. *Free Radic. Biol. Med.* **34**, 23-32.
Dalle-Donne, I., Rossi, R., Giustarini, D., Colombo, R. and Milzani, A. (2003b). Actin S-glutathionylation: evidence against a thiol-disulphide exchange mechanism. *Free Radic. Biol. Med.* **35**, 1185-1193.
Dean, J. B. (2010). Hypercapnia causes cellular oxidation and nitrosation in addition to acidosis: implications for CO_2 chemoreceptor function and dysfunction. *J. Appl. Physiol.* **108**, 1786-1795.
Denicola, A., Freeman, B. A., Trujillo, M. and Radi, R. (1996). Peroxynitrite reaction with carbon dioxide/bicarbonate: kinetics and influence on peroxynitrite-mediated oxidations. *Arch. Biochem. Biophys.* **333**, 49-58.
Dickson, A. G. (1990). Standard potential of the reaction: $AgCl(s) + 1/2H_2(g) = Ag(s) + HCl(aq)$, and the standard acidity constant of the ion HSO_4^- in synthetic sea water from 273.15 to 318.15. *J. Chem. Thermodyn.* **22**, 113-127.
Dickson, A. G., Sabine, C. L. and Christian, J. R. (2007). Guide to best practices for ocean CO_2 measurements. *PICES Special Publication* **3**, 191 pp.
Doney, S. C., Fabry, V. J., Feely, R. A. and Kleypas, J. A. (2009). Ocean acidification: the other CO_2 problem. *Annu. Rev. Mar. Sci.* **1**, 169-192.
English, T. E. and Storey, K. B. (2003). Freezing and anoxia stresses induce expression of metallothionein in the foot muscle and hepatopancreas of the marine gastropod *Littorina littorea*. *J. Exp. Biol.* **206**, 2517-2524.
Fang, F. C. (2004). Antimicrobial reactive oxygen and nitrogen species: concepts and controversies. *Nat. Rev. Microbiol.* **2**, 820-832.
Funato, Y. and Miki, H. (2007). Nucleoredoxin, a novel thioredoxin family member involved in cell growth and differentiation. *Antioxid. Redox Signal.* **9**, 1035-1057.
Glickman, M. H. and Ciechanover, A. (2002). The ubiquitin-proteasome proteolytic pathway: destruction for the sake of construction. *Physiol. Rev.* **82**, 373-428.
Go, Y. M. and Jones, D. P. (2008). Redox compartmentalization in eukaryotic cells. *Biochim. Biophys. Acta* **1780**, 1273-1290.
Gutierrez, J. L., Jones, C. G., Strayer, D. L. and Iribarne, O. O. (2003). Mollusks as ecosystem engineers: the role of shell production in aquatic habitats. *Oikos* **101**, 79-90.
Gutowska, M. A., Pörtner, H. O. and Melzner, F. (2008). Growth and calcification in the cephalopod *Sepia officinalis* under elevated seawater pCO_2. *Mar. Ecol. Prog. Ser.* **373**, 303-309.
Halliwell, B. and Gutteridge, J. M. C. (1999). *Free Radicals in Biology and Medicine*. Oxford and New York: Oxford University Press.
Hubertz, E. and Cahoon, L. (1999). Short-term variability of water quality parameters in two shallow estuaries of North Carolina. *Estuaries Coasts* **22**, 814-823.
IPCC (2007). *Climate Change 2007 – The Physical Science Basis*. Cambridge: Cambridge University Press.
Ishii, T. and Yanagawa, T. (2007). Stress-induced peroxiredoxins. In *Peroxiredoxin Systems*, Vol. 44 (ed. L. Flohé and J. R. Harris), pp. 375-384. New York: Springer.
Jackson, J. B. C. (2008). Ecological extinction and evolution in the brave new ocean. *Proc. Natl. Acad. Sci. USA* **105**, 11458-11465.
Jackson, J. B. C., Kirby, M. X., Berger, W. H., Bjorndal, K. A., Botsford, L. W., Bourque, B. J., Bradbury, R. H., Cooke, R., Erlandson, J., Estes, J. A. et al. (2001). Historical overfishing and the recent collapse of coastal ecosystems. *Science* **293**, 629-638.
Kirby, M. X. (2004). Fishing down the coast: historical expansion and collapse of oyster fisheries along continental margins. *Proc. Natl. Acad. Sci. USA* **101**, 13096-13099.
Koo, K. H., Lee, S., Jeong, S. Y., Kim, E. T., Kim, H. J., Kim, K., Song, K. and Chae, H. Z. (2002). Regulation of thioredoxin peroxidase activity by C-terminal truncation. *Arch. Biochem. Biophys.* **397**, 312-318.
Kossinova, O. A., Malygin, A. A., Babailova, E. S. and Karpova, G. G. (2008). Binding of human ribosomal protein p40 and its truncated mutants to the small ribosomal subunit. *Mol. Biol.* **42**, 911-916.
Lannig, G., Eilers, S., Pörtner, H. O., Sokolova, I. M. and Bock, C. (2010). Impact of ocean acidification on energy metabolism of oyster, *Crassostrea gigas* – changes in metabolic pathways and thermal response. *Mar. Drugs* **8**, 2318-2339.
Levraut, J., Iwase, H., Shao, Z. H., Vanden Hoek, T. L. and Schumacker, P. T. (2003). Cell death during ischemia: relationship to mitochondrial depolarization and ROS generation. *AJP-Heart Circ. Physiol.* **284**, H549-H558.
Lewis, E. and Wallace, D. W. R. (1998). Program developed for CO_2 system calculations. ORNL/CDIAC-105. Oak Ridge, TN: Carbon Dioxide Information Analysis Center, Oak Ridge National Laboratory, US Department of Energy. http://www.ecy.wa.gov/programs/eap/models.html
Lockwood, A. P. M. (1976). Physiological adaptation to life in estuaries. In *Adaptation to Environment* (ed. R. C. Newell), pp. 315-392. London and Boston: Butterworth.
Meli, R., Nauser, T., Latal, P. and Koppenol, W. (2002). Reaction of peroxynitrite with carbon dioxide: intermediates and determination of the yield of CO_2. *J. Biol. Inorg. Chem.* **7**, 31-36.
Meyer, Y., Buchanan, B. B., Vignols, F. and Reichheld, J. P. (2009). Thioredoxins and glutaredoxins: unifying elements in redox biology. *Annu. Rev. Genet.* **43**, 335-367.
Michaelidis, B., Ouzounis, C., Paleras, A. and Pörtner, H. O. (2005). Effects of long-term moderate hypercapnia on acid-base balance and growth rate in marine mussels *Mytilus galloprovincialis*. *Mar. Ecol. Prog. Ser.* **293**, 109-118.
Miller, A. W., Reynolds, A. C., Sobrino, C. and Riedel, G. F. (2009). Shellfish face uncertain future in high CO_2 world: influence of acidification on oyster larvae calcification and growth in estuaries. *PLoS ONE* **4**, e5661.
Millero, F. J., Graham, T. B., Huang, F., Bustos-Serrano, H. and Pierrot, D. (2006). Dissociation constants of carbonic acid in seawater as a function of salinity and temperature. *Mar. Chem.* **100**, 80-94.
Mohazzab, K. M., Kaminski, P. M. and Wolin, M. S. (1994). NADH oxidoreductase is a major source of superoxide anion in bovine coronary artery endothelium. *Am. J. Physiol. Heart Circ. Physiol.* **266**, H2568-H2572.
Murphy, M. P. (2009). How mitochondria produce reactive oxygen species. *Biochem. J.* **417**, 1-13.
Pannekoek, W. J., Kooistra, M. R., Zwartkruis, F. J. and Bos, J. L. (2009). Cell–cell junction formation: the role of Rap1 and Rap1 guanine nucleotide exchange factors. *Biochim. Biophys. Acta* **1788**, 790-796.
Perkins, E. J. (1974). *The Biology of Estuaries and Coastal Waters*. London: Academic Press.
Pörtner, H. O., Langenbuch, M. and Reipschläger, A. (2004). Biological impact of elevated ocean CO_2 concentrations: lessons from animal physiology and earth history. *J. Oceanogr.* **60**, 705-718.
Pritchard, D. W. (1967). What is an estuary: physical viewpoint. In *Estuaries* (ed. G. H. Lauff), pp. 3-5. Washington, DC: American Association for the Advancement of Science.
Ries, J. B., Cohen, A. L. and McCorkle, D. C. (2009). Marine calcifiers exhibit mixed responses to CO_2-induced ocean acidification. *Geology* **37**, 1131-1134.
Ringwood, A. H. and Keppler, C. J. (2002). Water quality variation and clam growth: is pH really a non-tissue in estuaries. *Estuaries* **25**, 901-907.
Rosa, R. and Seibel, B. A. (2008). Synergistic effects of climate-related variables suggest future physiological impairment in a top oceanic predator. *Proc. Natl. Acad. Sci. USA* **105**, 20776-20780.
Schulte, D. M., Burke, R. P. and Lipcius, R. N. (2009). Unprecedented restoration of a native oyster metapopulation. *Science* **325**, 1124-1128.
Sheehan, D. (2007). The potential of proteomics for providing new insights into environmental impacts on human health. *Rev. Environ. Health* **22**, 175-194.
Starkov, A. A. (2006). Protein-mediated energy-dissipating pathways in mitochondria. *Chem. Biol. Interact.* **163**, 133-144.
Stohs, S. J. and Bagchi, D. (1995). Oxidative mechanisms in the toxicity of metal ions. *Free Radic. Biol. Med.* **18**, 321-336.
Tell, G. (2006). Early molecular events during response to oxidative stress in human cells by differential proteomics. In *Redox Proteomics: From Protein Modifications to Cellular Dysfunction and Diseases* (ed. I. Dalle-Donne, A. Scaloni and D. A. Butterfield), pp. 369-397. Hoboken, NJ: John Wiley & Sons, Inc.
Tomanek, L. (2011). Environmental proteomics: changes in the proteome of marine organisms in response to environmental stress, pollutants, infection, symbiosis and development. *Annu. Rev. Mar. Sci.* **3**, 373-399.
Tomanek, L. and Zuzow, M. J. (2010). The proteomic response of the mussel congeners *Mytilus galloprovincialis* and *M. trossulus* to acute heat stress: implications for thermal tolerance and metabolic costs of thermal stress. *J. Exp. Biol.* **213**, 3559-3574.
Worm, B., Hilborn, R., Baum, J. K., Branch, T. A., Collie, J. S., Costello, C., Fogarty, M. J., Fulton, E. A., Hutchings, J. A., Jennings, S. et al. (2009). Rebuilding global fisheries. *Science* **325**, 578-585.